

# Effect of VA/RA on Oxidative Damage Induced by Hydrogen Peroxide in Primary Duck Intestinal Epithelial Cells

**Chao Zheng**

Hubei Academy of Agricultural Sciences

**Wen Zhuo Wei**

Hubei Academy of Agricultural Sciences

**Yan Wu**

Hubei Academy of Agricultural Sciences

**Zhenhua Liang**

Hubei Academy of Agricultural Sciences

**Jinsong Pi**

Hubei Academy of Agricultural Sciences

**Jingbo Liu**

Southwest University of Science and Technology

**Hao Zhang** (✉ [15172520011@163.com](mailto:15172520011@163.com))

Hubei Academy of Agricultural Sciences

---

## Research Article

**Keywords:** Vitamin A, Retinoic acid, Oxidative stress, PPAR, Nrf2/HO-1, Intestinal barrier

**Posted Date:** September 13th, 2021

**DOI:** <https://doi.org/10.21203/rs.3.rs-871297/v1>

**License:**   This work is licensed under a Creative Commons Attribution 4.0 International License.

[Read Full License](#)

---

# Abstract

**Background:** Vitamin A (VA) is an essential fat-soluble vitamin that contributes to the normal metabolism of intestinal epithelial cells (IEC), fights infections and enhances immunity. Retinoic acid (RA) is the physiological metabolite of VA, which is increased under oxidative stress and has an important physiological function. We studied the protective mechanism of VA/RA in H<sub>2</sub>O<sub>2</sub>-induced oxidative stress in primary duck IECs. Cells were distributed into 5 groups: blank control group (CG1), positive control group (CG2), high concentration retinoic acid group (TG1) (VA:RA=1 × 10<sup>-8</sup> M:3 × 10<sup>-8</sup> M), equal concentration retinoic acid group (TG2) (VA:RA=2 × 10<sup>-8</sup> M:2 × 10<sup>-8</sup> M), and low concentration retinoic acid group (TG3) (VA:RA=3 × 10<sup>-8</sup> M:1 × 10<sup>-8</sup> M). The blank control group had no treatment, and the positive control group and the treatment groups were all treated with 50 μM H<sub>2</sub>O<sub>2</sub> to induce oxidative stress. Each group had 3 replicates. RNA-Seq was used to screen differentially expressed genes, KEGG functional annotation and GO analysis were performed and the results were verified by qRT-PCR. The cell viability was quantified by the CCK-8 assay. Intestinal barrier integrity and tight junction permeability were measured by transepithelial electrical resistance (TEER).

**Results:** An RNA-Seq analysis showed that treatment with VA/RA altered the expression of genes involved in the cell adhesion, immune response, metabolism and cell regulation. Our results suggest that abnormal the PPAR $\gamma$  expression may be involved in H<sub>2</sub>O<sub>2</sub>-induced oxidative stress and in the therapeutic mechanism of VA/RA treatment. Treatment with 50 μM H<sub>2</sub>O<sub>2</sub> significantly decreased live cell numbers compared with those in CG1. Compared with those in CG2, the cell viability and TEER in the TGs were significantly improved (P < 0.05). As the RA concentration increased, the relative expression of Nrf2 and HO-1 increased (P < 0.05). The TGs had higher expression levels of ZO-1, claudin-1 and Occludin than CG2 (P < 0.05).

**Conclusions:** VA and its derivative RA relieve intestinal epithelial barrier dysfunction induced by H<sub>2</sub>O<sub>2</sub>, the PPAR and Nrf2/HO-1 signaling pathway may participate these proses.

## Introduction

Vitamin A (VA), also known as retinol, is an essential fat-soluble vitamin. Retinol is oxidized to form retinal under the action of retinol dehydrogenase, and retinal is irreversibly oxidized by retinal dehydrogenase to form retinoic acid. Retinoic acid (RA) is a VA Metabolite and is responsible for most of the physiological functions of vitamin A; RA contributes to the normal metabolism of intestinal epithelial cells, fights infections and enhances immunity [1–3]. Recent studies have found that VA and RA play an important role in enhancing the barrier of animal intestinal epithelial cells, improving the intestinal flora, and promoting the expression of tight junction proteins [4, 5]. IEC not only have an absorptive function but also act as a physical barrier between the body and the intestinal flora. The tight junctions between IEC form a tight barrier that prevents pathogens and toxins from invading the body from the intestinal lumen, and proper epithelial barrier maturation is essential for intestinal defense and homeostasis [6]. IEC

maintain host-microbe interactions and tissue homeostasis, are a key mediator of intestinal homeostasis, and establish an immune environment that allows symbiotic bacteria to colonize [7]. Under stress, the intestine is the first organ to become ischemic and the last organ recover [8]. The impact of stress on intestinal health should be examined. Therefore, protecting the intestinal epithelial barrier is a potential goal for the prevention or treatment of intestinal diseases. Studies on vitamin A and retinoic acid have shown that they are related to the tight junction function of the intestine. However, the mechanism of VA/RA involved in barrier function under stress is still unclear. To further study the relationship between retinoic acid metabolism and intestinal health, we induced oxidative stress by H<sub>2</sub>O<sub>2</sub> and established an oxidative stress model [9]. Different concentrations of VA/RA were added, and cell viability was measured by CCK-8 assays. The cellular barrier function of primary IEC from ducks was evaluated by measuring transmembrane resistance. RNA-Seq was used to screen differentially expressed genes, KEGG function annotation and GO analysis were performed and the results verified by qRT-PCR. Our findings indicated that abnormalities of the PPAR signaling pathway may be related to oxidative stress and VA and its derivative RA relieve intestinal epithelial barrier dysfunction induced by H<sub>2</sub>O<sub>2</sub>.

## Materials And Methods

### IEC culture and treatment

The IEC, primary cells isolated from Jingjiang duck embryos at embryonic day 26 and prepared following the method described in our previous studies [9]. Cells were grown in Dulbecco's modified Eagle's medium/F12 (Sigma-Aldrich, Louis, MO) containing 5% FBS (Mediatech. Inc., Manassas, VA), 1% penicillin-streptomycin (Sigma-Aldrich, St. Louis, MO), and 100 ng/mL epidermal growth factor (Rocky Hill, NJ). Cells were incubated at 5% CO<sub>2</sub>, and 37°C in 12-well cell culture dishes (Sangon, Shanghai, China) at a density of  $3 \times 10^5$  cells/cm<sup>2</sup>. The medium was changed every 36 h to maintain logarithmic growth. Cells were distributed into 5 groups after 36 h growth: blank control group (CG1), positive control group (CG2), high concentration retinoic acid group (TG1) (VA:RA =  $1 \times 10^{-8}$  M: $3 \times 10^{-8}$  M), equal concentration retinoic acid group (TG2) (VA:RA =  $2 \times 10^{-8}$  M: $2 \times 10^{-8}$  M), and low concentration retinoic acid group (TG3) (VA:RA =  $3 \times 10^{-8}$  M: $1 \times 10^{-8}$  M). The blank control group without any treatment, the positive control group and the treatment groups were all treated with 50 μM H<sub>2</sub>O<sub>2</sub> to induce oxidative stress. Each treatment had 3 replicates and each replicate had 3 wells.

### Cell morphology and proliferation

Cells were seeded in 96-well plates ( $2 \times 10^3$  cells/well). After the completion of treatment, 20 μL of Cell Counting Kit-8 (CCK-8; BS350A, Biosharp, China) was added to each well. After incubation for 4 h, the absorbance was measured at 450 nm with a microplate reader (Victor X5, PerkinElmer, Singapore). The cell viability percentage was calculated using the following formula: cell viability = (mean absorbance in the test wells) / (mean absorbance in the control well) × 100%.

# Measurements of IEC oxidative stress index induced by H<sub>2</sub>O<sub>2</sub>

After completion of treatments, the media was removed and cells washed twice with PBS. Cells were harvested in a 1.5mL centrifuge tube, add 200  $\mu$ L RIPA lysis buffer, lyse on ice for 30 min, centrifuge at 12000 rpm for 10 min, and take the supernatant. Content of malondialdehyde (MDA), activity of total antioxidant capacity (T-AOC) and total superoxide dismutase (T-SOD) were measured by colorimetric method (UV-2550, Shimadzu, Japan) with commercial assay kits (Nanjing Jiancheng institute of Bioengineering, Jiangsu, China) according to the manufacturer's instructions.

## Measurement of transepithelial electrical resistance (TEER)

The TEER was measured using an epithelial volt-ohm meter with a chopstick electrode (Millicell ERS-2, Millipore, Billerica, MA). The cells were seeded in Transwell® 6-well plates (Costar 3412, Corning, NY). The electrode was immersed at a 90° angle with one tip in the basolateral chamber and the other in the apical chamber. TEER value calculation: TEER value ( $\Omega \cdot \text{cm}^2$ ) = (cell growth hole value - blank hole value)  $\times$  micropore area. The microwell area of the insert area of the Transwell® 6-well cell culture plate was 4.67cm<sup>2</sup>.

## RNA extraction

Total RNA was isolated at the end of treatment using the TRIzol® assay (Invitrogen, Carlsbad, CA) and then treated with RQ1 DNase (Promega, Madison, WI). RNA integrity was assessed using the Agilent Bioanalyzer 2100 system (Agilent Technologies, CA). cDNA was synthesized using a Thermo® RtAid First Strand cDNA Synthesis Kit (Thermo Fisher Scientific, Waltham, MA) in a volume of 40  $\mu$ L.

## RNA sequencing

Three samples were randomly selected from each group for sequencing. An NEB Next Ultra RNA Library Preparation Kit (Illumina, San Diego, CA) was used to generate a sequence library with 3  $\mu$ g RNA for each sample. mRNA was purified with poly-T oligomer magnetic beads. The mRNA was purified cut into small pieces, and the cleaved RNA fragments were reverse transcribed into cDNA. Single-end sequencing of each library was applied to the HiSeq 2000 platform by Novogene Inc. (Tianjin, China). Using the TopHat program, we mapped all clean reads obtained from RNA-Seq with three mismatched Anas platyrhynchos genome constructs, and the annotation data were downloaded from [www.ncbi.nlm.nih.gov/genome](http://www.ncbi.nlm.nih.gov/genome). For comparison of the abundance of mRNA, the read count of each mRNA was normalized to RPKM (reads per kilobase of a gene per million reads). RPKM  $\geq$  100 was used to identify differentially expressed genes between the two groups, with a P value < 0.01.

## Real-time quantitative RT-PCR

Quantitative real-time PCR was performed using a LightCycler® 96 system (Roche, Life Science) with the SYBR® PrimeScript™ RT-PCR Kit (Roche, Mannheim, Germany). There were three replicates for each

sample. All primers for the genes of interest were designed with Premier 5 and are shown in Table 1. Relative mRNA expression was calculated according to the  $2^{-\Delta\Delta Ct}$  method.

Table 1  
The primers used in this study.

Gene name	Primer sequence (5' to 3')
ACSL1	Sense: CTCTGCGT TACTCCACCG
	Antisense: GCATAGCATCCCTGTTTCG
ACSL5	Sense: AACCCAACCAACCTTATC
	Antisense: TGTCACAAATCACTACGC
PPARG	Sense: TAACGCTCCTGAAATACGGT
	Antisense: GAACTTCACAGCGAACTCAA
Nrf2	Sense: TGTTGAATCATCTGCCTGTG
	Antisense: TTGTGAACGGTGCTTTGG
HO-1	Sense: TGCCTACACTCGCTATCTGG
	Antisense: CGTTCTCCTGGCTCTTTGA
ZO-1	Sense: GCACCGAAGCCTACACTCA
	Antisense: CGGTAATACTCTTCATCTTCTT
Claudin-1	Sense: TGACCAGGTGAAGAAGATGC
	Antisense: GGGTGGGTGGATAGGAAGT
Occludin	Sense: GCTGGGCTACAACCTACGGGT
	Antisense: ACGATGGAGGCGATGAGC
$\beta$ -Actin	Sense: GCTATGTCGCCCTGGATTT
	Antisense: GGATGCCACAGGACTCCATAC

## Statistical analysis

SPSS 23.0 software (IBM, Inc., NY, USA) was used for data analysis, and one-way ANOVA was used for variance analysis. Duncan's method was used for multiple comparisons of the mean values between the groups when the differences were significant, and the results are expressed as the mean  $\pm$  SD. Differences were considered significant when  $P < 0.05$ .

## Results

### Survival of IECs after oxidative damage

Nonchallenged cells were observed after 36 h of culture and formed a regular monolayer pattern (Fig. 1.A). Exposure to  $H_2O_2$  without any treatment resulted in numerous dead or disrupted cells (Fig. 1.B) compared with those in the control, nonchallenged cells (Fig. 1.A). Exposure to  $H_2O_2$  and treated with high concentrations of RA showed a small amount of cell metabolites floating and normal cell morphology (Fig. 1.C). Those exposure to  $H_2O_2$  and treated with equal, low concentration of RA, floating cell fragments can be observed, and its intercellular space enlarged. (Fig. 1. D and E).

The cell viability was quantified by CCK-8 assays and is shown in Fig. 2. The oxidative stress model was established according to the method mentioned above. Assuming that the viability of CG1 cell was 100%, a final concentration of 50  $\mu M$   $H_2O_2$  was added to the culture medium to establish the oxidative stress model. When the cell viability of CG2 dropped to approximately 80%, the oxidative stress model has been successfully established. Compared with that of CG2 (Fig. 2), the cell viability of TG1, TG2 and TG3 was significantly improved ( $P < 0.05$ ). Treatment with high concentrations of RA had an obvious protective effect.

## Effects of VA/RA on antioxidant capacity

As shown in Table 2, significant differences in T-AOC, T-SOD and MDA levels were observed between the CGs and those in the TGs. T-AOC activity of TG2 and TG3 was higher than that of other groups ( $P < 0.05$ ). Compared with CG2, TG1 had lower level of MDA ( $P < 0.05$ ). T-SOD activity of TG3 was higher than that of other groups ( $P < 0.05$ ).

Table 2  
DEGs of cell adhesion molecules

Gene_id	Expressed in CG2	Expressed in TG1	Expressed in TG2	Expressed in TG3	gene_name
101799657	433.09	702.72	780.80	934.38	RUNX1
101791636	972.72	1372.88	1593.58	1619.18	JAM3
101803496	487.47	977.48	1106.08	995.05	TIAM1
101795217	10400.21	12598.66	14548.31	14718.14	ACTN1
101791510	2516.92	3230.85	3456.62	3713.51	PARD6B
101791567	328.23	457.14	453.04	560.77	IGSF5
101799109	4031.63	4912.55	5590.81	5425.25	MAP3K5
101801136	6468.77	7380.22	8279.38	8516.91	PRKCI
101803417	2686.21	3574.38	3705.84	3695.80	AMOTL1
101797155	543.221	309.29	359.14	356.62	MPDZ
101803710	1003.32	1195.72	1269.48	1358.81	PRKAG2
101802851	41.26	77.24	77.66	128.99	CLDN4
101791936	395.34	520.68	572.45	557.54	LOC101791936
101790465	20.31	54.50	43.09	63.50	LOC101790465
101801218	153.14	255.24	254.96	268.74	LOC101801218
101793656	1328.82	1696.27	1822.72	1770.73	MAP3K1
101800296	2125.94	2609.28	2510.24	2602.50	RAP1A
106014700	3386.153	2853.70	2391.75	2731.89	SLC9A3R1
101792652	45.08	75.06	66.36	86.18	BVES
101796398	475.94	335.45	352.28	360.73	GATA4
101795656	4844.51	4165.15	5280.73	5509.47	ACTR3
101798527	1163.09	1361.82	1425.80	1363.29	PPP2R2D
101802171	1.5966	12.63	12.89	9.79	LOC101802171
101801112	760.9386	876.77	995.91	875.07	CGNL1
101803563	392.577	112.06	190.91	200.90	MYH11
101794204	1175.774	2130.88	1845.72	1930.56	MICALL2

Gene_id	Expressed in CG2	Expressed in TG1	Expressed in TG2	Expressed in TG3	gene_name
101797289	1853.39	1147.93	1191.99	1287.66	LOC101797289
101797741	9994.628	19896.90	19585.97	24172.14	CLDN1
101799368	1979.942	1098.24	1416.19	1478.66	MYL9
101790688	174.5561	377.97	354.95	487.95	CLDN5
101794867	67.97059	188.21	142.99	118.74	CLDN18
101802565	2315.09	1775.78	1867.11	1781.55	CGN
101794832	1284.76	1601.75	1671.98	1563.48	ARHGEF18
101796626	4151.58	7884.30	6790.85	8512.31	JUN
101794726	3451.32	2716.95	3115.04	2999.10	RDX
101797340	2625.15	3098.37	3145.67	3011.84	WASL
101790278	13647.68	18666.50	17850.12	21596.08	LOC101790278
101795602	147.76	68.16	83.95	101.61	LOC101795602
101800437	78918.93	60067.92	67740.71	71608.55	ACTB

## VA/RA increases the TEER of IEC monolayers subjected to an oxidative stress stimulus

TEER was used to measure the integrity of the cell monolayer and was evaluated before and after all treatments. Previous studies have shown that H<sub>2</sub>O<sub>2</sub> can increase the permeability of intestinal tight junctions. We investigated the effect of VA/RA and H<sub>2</sub>O<sub>2</sub> on epithelial cell integrity by measuring TEER at 0, 12 and 24 h. H<sub>2</sub>O<sub>2</sub> treatment significantly decreased TEER (P < 0.05) after 12 h, and this decrease continued until 24 h (Fig. 3). However, the addition of VA/RA significantly increased TEER (P < 0.05), suggesting that VA/RA combined treatment can increase intestinal epithelial permeability.

### Principal component analysis

Principal component analysis (PCA) is also commonly used to evaluate differences between groups and sample duplication within groups. PCA uses linear algebra calculation methods to reduce dimensionality and extract principal components of tens of thousands of genetic variables. We performed PCA on the fragments per kilobase per million (FPKM) of all samples, as shown in the Fig. 4. Under ideal conditions, in the PCA chart, the samples between the groups should be scattered, and the samples within the groups should be clustered together. We found that TG1 had the greatest degree of dispersion compared with CG1 and CG2. Therefore, we choose TG1 as the main research object.

# KEGG enrichment analysis of differentially expressed genes

To explore the effect of VA/RA treatment, we examined the enriched DEGs between CG2 and TGs. We found that the VA/RA processing method changed the pathways related to cell adhesion molecules and the PPAR signaling pathway (Fig. 5).

## Analysis of differential gene expression related to cell adhesion molecules and the PPAR signaling pathway.

Comparing the TGs with CG2, we identified 40 differentially expressed genes among cell adhesion molecules, including 30 genes with upregulated expression and 10 downregulated expression (Fig. 6.A). In total, 27 DEGs were identified among the TGs and CG2 in the PPAR signaling pathway: 22 with upregulated and 5 with downregulated expression (Fig. 6.B). All of the DEGs are listed in the Table 2 and Table 3.

Table 3  
DEGs of PPAR signaling pathway

gene_id	Expressed in CG2	Expressed in TG1	Expressed in TG2	Expressed in TG3	gene_name
101801349	8826.15	61558.33	46516.78	38820.17	SCD
101801834	65.86	781.70	1140.56	970.70	ACSL5
101792626	36.33	255.63	471.91	487.49	LOC101792626
101799889	2276.75	7774.45	7049.63	6406.19	ACSBG2
101799911	1879.02	4245.37	3536.58	3488.32	PLIN2
101798758	1818.79	3124.72	4434.30	3600.73	FADS2
101798039	1160.46	2971.77	2443.51	2628.27	ACSL1
101804521	255.98	1105.48	626.90	547.48	GK
101799612	867.68	1607.27	1587.92	1437.90	CPT1A
101792429	332.78	659.85	604.69	549.72	PPARG
101800606	2690.51	4070.02	3716.41	3517.34	ACOX1
101797549	457.02	1588.39	1609.18	2396.16	ANGPTL4
101796118	2488.63	3715.83	4042.74	3465.24	ACSL3
101793392	69.43	107.46	185.17	151.51	LOC101793392
101797590	11894.55	7049.87	8723.36	8773.60	UBC
101789691	1737.319	2519.92	2320.97	2212.06	NR1H3
101790559	2174.616	1429.36	1490.10	1632.95	ILK
101797140	3528.607	5151.82	4970.13	4864.95	APOA1
101796218	92.14506	137.01	174.60	164.54	LPL
101802067	643.8781	485.98	449.58	465.69	PLTP
101798010	5814.069	6842.19	7002.18	6964.23	PDPK1
101793637	37.7875	8.42	18.90	14.55	PCK1
101799068	17760.32	31207.44	24473.29	30081.50	LOC101799068
101798298	47.64614	11.14	18.86	21.03	LOC101798298
101798003	1008.136	1135.18	1191.87	1188.99	ACSL4
101805272	3280.113	2982.71	3782.86	3744.21	DBI

# Dysregulated genes involved in the PPAR signaling pathway

KEGG analysis showed that the PPAR signaling pathway was involved in the oxidative stress process, and VA/RA treatment significantly restored this pathway. Regarding genes in the PPAR signaling pathway, we identified long-chain fatty acid CoA ligase 1 (ACSL1), peroxisome proliferator activated receptor-gamma (PPAR- $\gamma$ /PPARG) and long-chain fatty acid CoA ligase 5 (ACSL5). The relative gene expression is shown in Fig. 7. The TGs had higher expression levels of PPARG, ACSL1 and ACSL5 than CG2 ( $P < 0.05$ ).

## Transcripts of antioxidative stress and intestinal barrier related genes after oxidative challenge

The antioxidative stress and intestinal barrier related genes expression is shown in Fig. 8. The qRT-PCR results showed that the relative expression levels of Nrf2/HO-1 were significantly reduced in CG2 compared with CG1 ( $P < 0.05$ ). As the RA levels increased, the relative expression of Nrf2 and HO-1 increased ( $P < 0.05$ ). The TGs had higher expression levels of ZO-1, claudin-1 and Occludin than CG2 ( $P < 0.05$ ).

## Discussion

In the early stage of raising caged laying ducks, the pressure level changed substantially, which not only caused a certain degree of liver tissue damage, but also increased the expression of inflammatory injury factors [10]. Our previous study found that during the peak of stress response in laying ducks, the content of VA/RA in serum changed. At the same time, the caged laying ducks showed intestinal barrier dysfunction, and the related genes affecting RA biosynthesis in the intestine changed. Therefore, we believe that VA/RA is related to intestinal barrier function. We designed the experiment to investigate the effect of VA on intestinal barrier function. VA is a multifunctional vitamin involved in a variety of biological processes. Its control of the immune system and function may not only be the most effective for development but also for protective or regulatory adaptive immunity [11]. This effect is especially important at the intestinal border where dietary vitamin A is first absorbed. Most of the effects of vitamin A are produced by its metabolite retinoic acid (RA). Li et al found that vitamin A increased Toll-like receptor 4 (TLR4) expression through its receptor, thereby enhancing intestinal barrier function in colonic mucosal cells, suggesting the connection between inflammation and VA supplementation [12].

Changes in organisms during stress are postulated to be linked to accumulating lipid peroxidation products, such as free radicals, peroxy radicals, hydroperoxides, aldehydes and ketones [13]. Lipid peroxidation is defined as a parameter of oxidative stress [14]. T-SOD acts as a catalyst in the removal of toxic superoxide radicals [15]. An elevated level of T-SOD activity is a defense mechanism against an increased level of free radicals under stressful conditions [16]. After H<sub>2</sub>O<sub>2</sub> treatment, significant differences in T-SOD, T-AOC and MDA levels were observed between the CG1 and those in the CG2. In this experiment, the activity of T-AOC and T-SOD was increased and the content of MDA was decreased in

cells treated with appropriate concentration of VA/RA, which proved that VA/RA improve the level of antioxidant in cells. It has been consistently reported that TEER is one of the most commonly used indicators for the permeability of intestinal epithelial cells [17, 18]. The enhancement of barrier function was manifested by the decrease of paracellular permeability and the increase of TEER. In the present study, we determined that the addition of VA/RA increased cell viability after oxidative stress stimulation. The TEER test showed that VA metabolism affected intestinal permeability. Primary IECs using duck embryos have basic structure, metabolism and functions comparable to intestinal epithelial cells in vivo and can be used as a good model for studying poultry gastrointestinal response mechanisms under stress conditions [9]. Oxidative stress generates a large amount of reactive oxygen species (ROS). Studies have shown that ROS can cause endoplasmic reticulum stress leading to apoptosis [19]. Destruction of the intestinal barrier function is related to intestinal epithelial cell apoptosis [20]. Studies have shown that vitamin A reverses LPS-induced intestinal barrier damage by increasing the expression of intestinal barrier proteins [21]. However, research on the specific regulatory mechanism is still very limited, and comprehensive, in-depth and continuous research is still needed. We used RNA-seq to screen differentially expressed genes, and study the protective mechanism of VA/RA on H<sub>2</sub>O<sub>2</sub>-induced oxidative stress in primary duck IECs.

Antioxidants and lipid peroxidation are key factors in the response to stress. Lipid peroxidation is defined as a parameter of oxidative stress. Peroxisome proliferator-activated receptors (PPARs) can regulate the function and expression of complex gene networks, such as energy homeostasis and inflammation [22, 23]. This family includes three known members: PPAR $\alpha$ , PPAR $\beta$  and PPAR $\gamma$ , also known as NR1C1, NR1C2 and NR1C3[24]. PPAR $\gamma$  is related to oxidative stress, and oxidative stress can activate a variety of transcription factors, including NF- $\kappa$ B, P53, PPAR  $\gamma$  and Nrf2 [25].

The role of PPAR $\gamma$  in oxidative stress is mainly to inhibit damage and promote cell survival, in this defense system, PPAR $\gamma$  does not act alone, but forms a positive feedback loop with Nrf2 to exert its anti-inflammatory effect and inhibit NF- $\kappa$ B pathway [26]. Nrf2 is a key transcription factor in oxidative stress that responds to cell damage induced by high levels of ROS. It binds to the antioxidant response element (ARE) and mediates the expression of heme oxygenase-1 (HO-1), which plays an important role in inhibiting cell oxidative damage and is the first line of defense against oxidative stress damage [27, 28]. HO-1 reduces oxidative stress, inflammation, and apoptosis by reducing the production of ROS [29]. PPAR $\gamma$  upregulates HO-1 expression and protects cells from endothelial cell toxicity induced by TNF- $\alpha$  [30]. Studies have shown that retinoic acid can reduce H<sub>2</sub>O<sub>2</sub>-induced cell oxidative stress damage by upregulating Nrf2/HO-1 expression, which is an important cytoprotective mechanism against oxidative damage [31, 32]. In this research, the relative gene expression levels of PPAR, Nrf2 and HO-1 in the TGs were significantly higher than those in the CG2. The results showed that treatment with VA/RA =  $1 \times 10^{-8}$  M:  $3 \times 10^{-8}$  M can improve the antioxidant function of IECs under oxidative stress, which may be achieved by regulating the PPAR-mediated Nrf2/HO-1 signaling pathway.

HO-1 is involved in endothelial barrier dysfunction induced by oxidative stress, such as intestinal epithelial dysfunction [33, 34]. Previous studies have found that HO-1 can protect intestinal epithelial cells

from oxidative damage by upregulating tight junction protein (TJP) levels [35, 36]. The integrity of epithelial structure and function depends on the normal function and regulation of tight junction proteins, including claudins and ZOs. Studies have shown that changes in ZO-1 and claudin-1 are related to intestinal epithelial dysfunction [21, 37]. KEGG pathway analysis revealed that the signaling pathways were mainly enriched in the categories of cell adhesion molecules, immune response and cell regulation. Cell adhesion molecules are involved in focal adhesion and tight junctions. Similarly, qRT-PCR results showed that H<sub>2</sub>O<sub>2</sub> stimulation can cause downregulation of ZO-1, claudin-1, and Occludin expression, which indicates that these TJP are essential in abnormal intestinal barrier function, and the addition of VA/RA leads to upregulation of TJP expression.

## Conclusions

Our findings indicated that abnormalities of the PPAR signaling pathway may be related to oxidative stress and VA and its derivative RA relieve intestinal epithelial barrier dysfunction induced by H<sub>2</sub>O<sub>2</sub>.

## Abbreviations

VA: Vitamin A; IEC: Intestinal epithelial cells; RA: Retinoic acid; TEER: Transepithelial electrical resistance; CCK-8: Cell Counting Kit-8; MDA: Malondialdehyde; T-AOC: Total antioxidant capacity; T-SOD: total superoxide dismutase; PCA: Principal component analysis; TLR4: Toll-like receptor 4; ROS: Reactive oxygen species; TJP: Tight junction protein.

## Declarations

## Ethics approval and consent to participate

The experiments were approved by the Ethics Committee of Hubei Academy of Agricultural Sciences according to Hubei Province Laboratory Animal Management Regulations – 2005. All operations complied with the Chinese guidelines for the ethical treatment of experimental animals.

## Consent for publication

All authors read and approved the final manuscript, and consent for publication.

## Availability of data and materials

The datasets of RNA-Seq generated for this study can be found in the Sequence Read Archive (SRA) database (Bioproject ID: PRJNA757931)

## Competing interests

The authors declare that the research was conducted in the absence of any commercial or financial relationships that could be construed as a potential conflict of interest.

## Fundings

This work was supported by grants from the National Natural Science Foundation (grant number: 31702157); China Agriculture Research System of MOF and MARA (grant number: CARS-42-47); and the Hubei Provincial scientific and technological innovation special project (grant numbers: 2020BBA034); Leading Talents Program of Hubei Academy of Agricultural Sciences (grant number: L2018017).

## Authors' Contributions

Hao Zhang and Yan Wu conceived and designed the experiments. Zhenhua Liang was responsible for sample preparation. Chao Zheng and Wenzhuo Wei analysed the data. Jinsong Pi and Jingbo Liu interpreted the results and contributed to edit the manuscript. Chao Zheng and Wenzhuo Wei wrote the paper.

## Acknowledgements

Not applicable.

## References

1. Uni Z, Zaiger G, Gal-Garber O, et al. Vitamin A deficiency interferes with proliferation and maturation of cells in the chicken small intestine. *British poultry science* 2000;41:410–5. <http://doi.org/10.1080/713654958>
2. Blaner WS, Li Y, Brun PJ, et al. Vitamin A Absorption, Storage and Mobilization. *Sub-cellular biochemistry* 2016;81:95–125. [http://doi.org/10.1007/978-94-024-0945-1\\_4](http://doi.org/10.1007/978-94-024-0945-1_4)
3. Cassani B, Villablanca EJ, De Calisto J, Wang S, Mora JR. Vitamin A and immune regulation: role of retinoic acid in gut-associated dendritic cell education, immune protection and tolerance. *Molecular aspects of medicine* 2012;33:63–76. <http://doi.org/10.1016/j.mam.2011.11.001>
4. Xiao S, Li Q, Hu K, et al. Vitamin A and Retinoic Acid Exhibit Protective Effects on Necrotizing Enterocolitis by Regulating Intestinal Flora and Enhancing the Intestinal Epithelial Barrier. *Archives of medical research* 2018;49:1–9. <http://doi.org/10.1016/j.arcmed.2018.04.003>

5. Xiao L, Cui T, Liu S, et al. Vitamin A supplementation improves the intestinal mucosal barrier and facilitates the expression of tight junction proteins in rats with diarrhea. *Nutrition* (Burbank, Los Angeles County, Calif.) 2019;57:97–108. <http://doi.org/10.1016/j.nut.2018.06.007>
6. Yamada S, Kanda Y. Retinoic acid promotes barrier functions in human iPSC-derived intestinal epithelial monolayers. *Journal of pharmacological sciences* 2019;140:337 – 44. <http://doi.org/10.1016/j.jphs.2019.06.012>
7. Peterson LW, Artis D. Intestinal epithelial cells: regulators of barrier function and immune homeostasis. *Nature reviews. Immunology* 2014;14:141–53. <http://doi.org/10.1038/nri3608>
8. Zou Y, Wei HK, Xiang QH, et al. Protective effect of quercetin on pig intestinal integrity after transport stress is associated with regulation oxidative status and inflammation. *The Journal of veterinary medical science* 2016;78:1487–94. <http://doi.org/10.1292/jvms.16-0090>
9. Zhang H, Chen F, Liang ZH, Wu Y, Pi JS. Isolation, culture, and identification of duck intestinal epithelial cells and oxidative stress model constructed. *In vitro cellular & developmental biology. Animal* 2019;55:733–40. <http://doi.org/10.1007/s11626-019-00388-7>
10. Zhang Y, Gu T, Tian Y, et al. Effects of cage and floor rearing system on the factors of antioxidant defense and inflammatory injury in laying ducks. *BMC genetics* 2019;20:103. <http://doi.org/10.1186/s12863-019-0806-0>
11. Larange A, Cheroutre H. Retinoic Acid and Retinoic Acid Receptors as Pleiotropic Modulators of the Immune System. *Annual review of immunology* 2016;34:369–94. <http://doi.org/10.1146/annurev-immunol-041015-055427>
12. Li Y, Gao Y, Cui T, et al. Retinoic Acid Facilitates Toll-Like Receptor 4 Expression to Improve Intestinal Barrier Function through Retinoic Acid Receptor Beta. *Cellular physiology and biochemistry: international journal of experimental cellular physiology, biochemistry, and pharmacology* 2017;42:1390 – 406. <http://doi.org/10.1159/000479203>
13. Bekenev V, Garcia A, Hasnulin V. Adaptation of Piglets Using Different Methods of Stress Prevention. *Animals: an open access journal from MDPI* 2015;5:349–60. <http://doi.org/10.3390/ani5020349>
14. Niki E. Lipid peroxidation products as oxidative stress biomarkers. *BioFactors* (Oxford, England) 2008;34:171–80. <http://doi.org/10.1002/biof.5520340208>
15. Rehman ZU, Meng C, Sun Y, et al. Oxidative Stress in Poultry: Lessons from the Viral Infections. *Oxidative medicine and cellular longevity* 2018;2018:5123147. <http://doi.org/10.1155/2018/5123147>
16. Meynaghizadeh-Zargar R, Sadigh-Eteghad S, Mohaddes G, Salehpour F, Rasta SH. Effects of transcranial photobiomodulation and methylene blue on biochemical and behavioral profiles in mice stress model. *Lasers in medical science* 2020;35:573–84. <http://doi.org/10.1007/s10103-019-02851-z>
17. Putt KK, Pei R, White HM, Bolling BW. Yogurt inhibits intestinal barrier dysfunction in Caco-2 cells by increasing tight junctions. *Food & function* 2017;8:406–14. <http://doi.org/10.1039/c6fo01592a>

18. Srinivasan B, Kolli AR, Esch MB, et al. TEER measurement techniques for in vitro barrier model systems. *Journal of laboratory automation* 2015;20:107–26.  
<http://doi.org/10.1177/2211068214561025>
19. Zeeshan HM, Lee GH, Kim HR, Chae HJ. Endoplasmic Reticulum Stress and Associated ROS. *International journal of molecular sciences* 2016;17:327. <http://doi.org/10.3390/ijms17030327>
20. Feng L, Chen S, Zhang L, Qu W, Chen Z. Bisphenol A increases intestinal permeability through disrupting intestinal barrier function in mice. *Environmental pollution (Barking, Essex: 1987)* 2019;254:112960. <http://doi.org/10.1016/j.envpol.2019.112960>
21. He C, Deng J, Hu X, et al. Vitamin A inhibits the action of LPS on the intestinal epithelial barrier function and tight junction proteins. *Food & function* 2019;10:1235–42.  
<http://doi.org/10.1039/c8fo01123k>
22. Desvergne B, Wahli W. Peroxisome proliferator-activated receptors: nuclear control of metabolism. *Endocrine reviews* 1999;20:649–88. <http://doi.org/10.1210/edrv.20.5.0380>
23. Varga T, Czimmerer Z, Nagy L. PPARs are a unique set of fatty acid regulated transcription factors controlling both lipid metabolism and inflammation. *Biochimica et biophysica acta* 2011;1812:1007–22. <http://doi.org/10.1016/j.bbadis.2011.02.014>
24. Berger J, Moller DE. The mechanisms of action of PPARs. *Annual review of medicine* 2002;53:409–35. <http://doi.org/10.1146/annurev.med.53.082901.104018>
25. Reuter S, Gupta SC, Chaturvedi MM, Aggarwal BB. Oxidative stress, inflammation, and cancer: how are they linked? *Free radical biology & medicine* 2010;49:1603–16.  
<http://doi.org/10.1016/j.freeradbiomed.2010.09.006>
26. Polvani S, Tarocchi M, Galli A. PPAR $\gamma$  and Oxidative Stress: Con( $\beta$ ) Catenating NRF2 and FOXO. *PPAR research* 2012;2012:641087. <http://doi.org/10.1155/2012/641087>
27. Zhang L, Qin Z, Li R, et al. The role of ANXA5 in DBP-induced oxidative stress through ERK/Nrf2 pathway. *Environmental toxicology and pharmacology* 2019;72:103236.  
<http://doi.org/10.1016/j.etap.2019.103236>
28. Taira J, Ogi T. Induction of Antioxidant Protein HO-1 Through Nrf2-ARE Signaling Due to Pteryxin in *Peucedanum Japonicum* Thunb in RAW264.7 Macrophage Cells. *Antioxidants (Basel, Switzerland)* 2019;8. <http://doi.org/10.3390/antiox8120621>
29. Wang Y, Yang C, Elsheikh NAH, et al. HO-1 reduces heat stress-induced apoptosis in bovine granulosa cells by suppressing oxidative stress. *Aging* 2019;11:5535–47.  
<http://doi.org/10.18632/aging.102136>
30. Park SY, Bae JU, Hong KW, Kim CD. HO-1 Induced by Cilostazol Protects Against TNF- $\alpha$ -associated Cytotoxicity via a PPAR- $\gamma$ -dependent Pathway in Human Endothelial Cells. *The Korean journal of physiology & pharmacology: official journal of the Korean Physiological Society and the Korean Society of Pharmacology* 2011;15:83–8. <http://doi.org/10.4196/kjpp.2011.15.2.83>
31. Chatterjee A, Chatterji U. All-Trans Retinoic Acid Ameliorates Arsenic-Induced Oxidative Stress and Apoptosis in the Rat Uterus by Modulating MAPK Signaling Proteins. *Journal of cellular biochemistry*

- 2017;118:3796–809. <http://doi.org/10.1002/jcb.26029>
32. Zhang H, Yuan B, Huang H, et al. Gastrodin induced HO-1 and Nrf2 up-regulation to alleviate H<sub>2</sub>O<sub>2</sub>-induced oxidative stress in mouse liver sinusoidal endothelial cells through p38 MAPK phosphorylation. *Brazilian journal of medical and biological research = Revista brasileira de pesquisas medicas e biologicas* 2018;51:e7439. <http://doi.org/10.1590/1414-431x20187439>
33. Wang N, Han Q, Wang G, et al. Resveratrol Protects Oxidative Stress-Induced Intestinal Epithelial Barrier Dysfunction by Upregulating Heme Oxygenase-1 Expression. *Digestive diseases and sciences* 2016;61:2522–34. <http://doi.org/10.1007/s10620-016-4184-4>
34. Wang N, Wang G, Hao J, et al. Curcumin ameliorates hydrogen peroxide-induced epithelial barrier disruption by upregulating heme oxygenase-1 expression in human intestinal epithelial cells. *Digestive diseases and sciences* 2012;57:1792–801. <http://doi.org/10.1007/s10620-012-2094-7>
35. Zhuang S, Yu R, Zhong J, Liu P, Liu Z. Rhein from *Rheum rhabarbarum* Inhibits Hydrogen-Peroxide-Induced Oxidative Stress in Intestinal Epithelial Cells Partly through PI3K/Akt-Mediated Nrf2/HO-1 Pathways. *Journal of agricultural and food chemistry* 2019;67:2519–29. <http://doi.org/10.1021/acs.jafc.9b00037>
36. He S, Guo Y, Zhao J, et al. Ferulic acid protects against heat stress-induced intestinal epithelial barrier dysfunction in IEC-6 cells via the PI3K/Akt-mediated Nrf2/HO-1 signaling pathway. *International journal of hyperthermia: the official journal of European Society for Hyperthermic Oncology, North American Hyperthermia Group* 2019;35:112–21. <http://doi.org/10.1080/02656736.2018.1483534>
37. Lin X, Jiang S, Jiang Z, Zheng C, Gou Z. Effects of equol on H<sub>2</sub>O<sub>2</sub>-induced oxidative stress in primary chicken intestinal epithelial cells. *Poultry science* 2016;95:1380–6. <http://doi.org/10.3382/ps/pew034>

## Figures

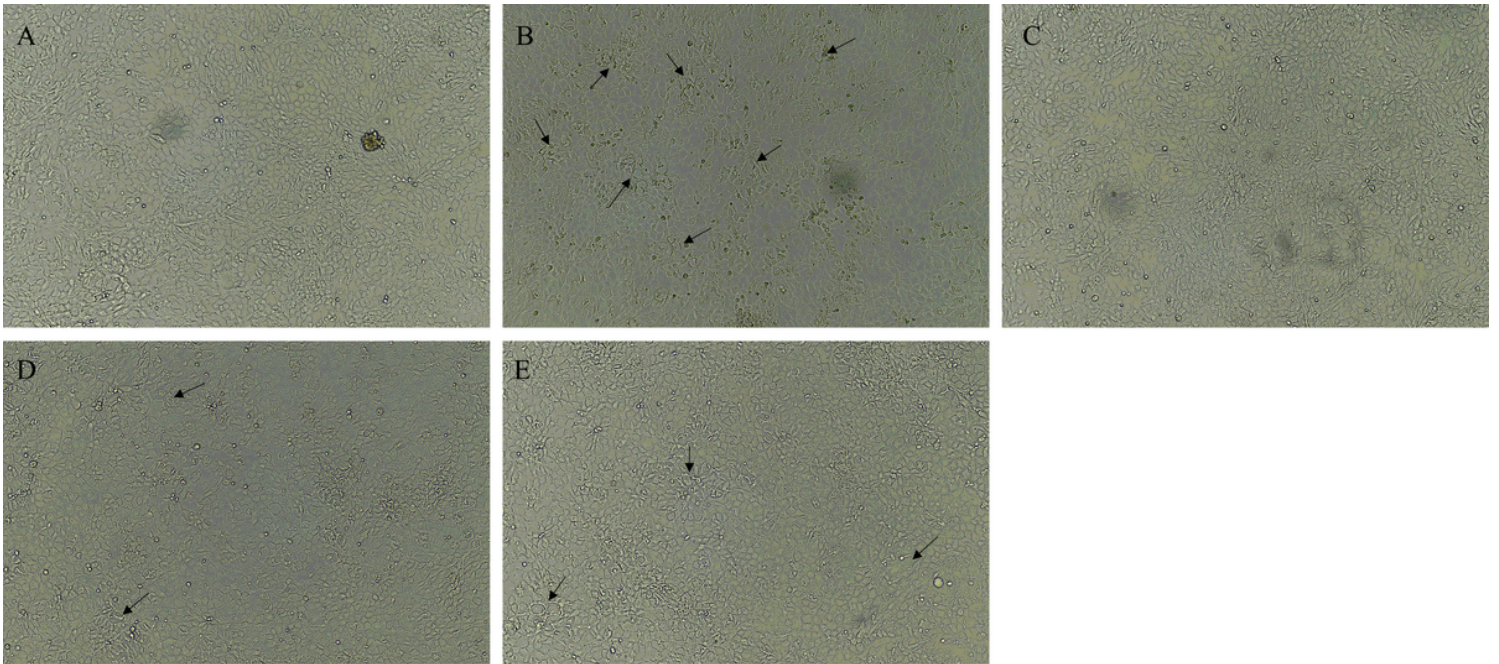


**Figure 1**

Morphological changes in IEC after challenge with H<sub>2</sub>O<sub>2</sub> and subsequent VA/RA treatment (×100). The arrows in the figure indicate cell floatation and intercellular space.

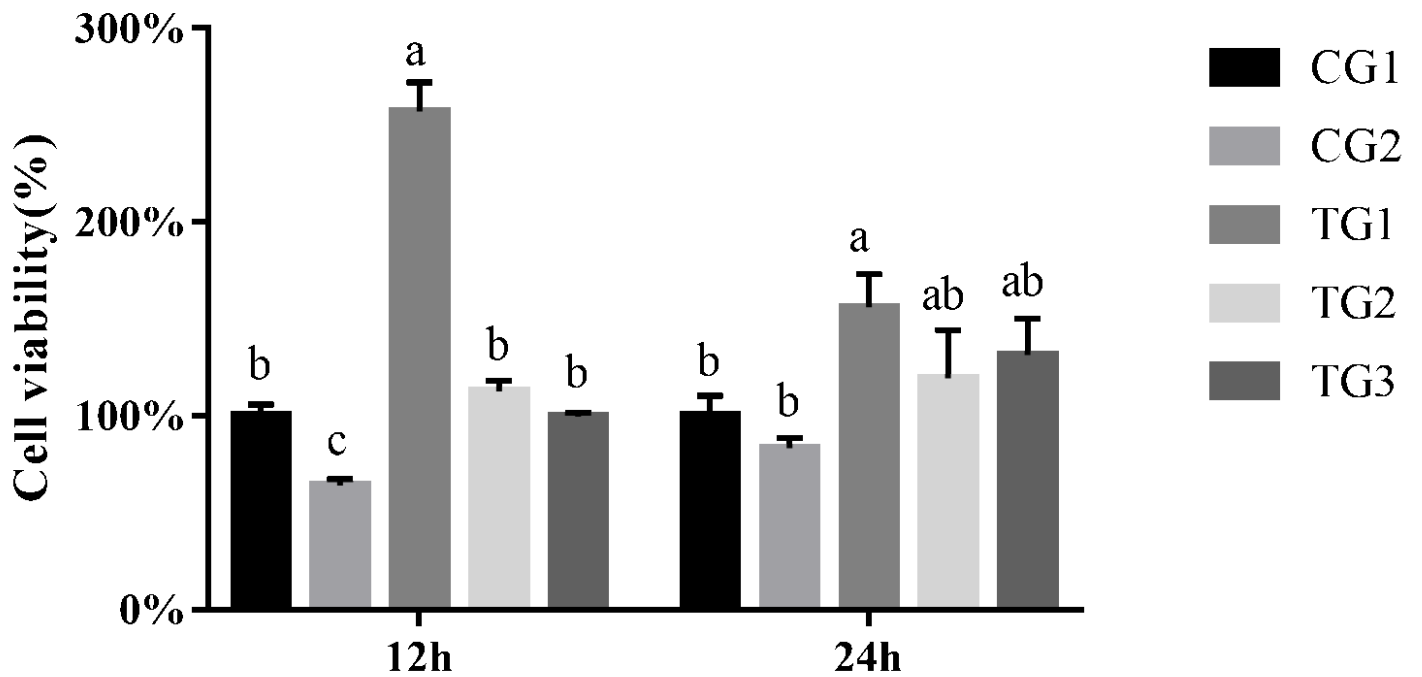


**Figure 2**

Effect of VA and its derivative RA on cell viability after H<sub>2</sub>O<sub>2</sub>-induced oxidative stress. Data are means  $\pm$  SD, n = 6. Bars with different letters indicate significant difference (P < 0.05).

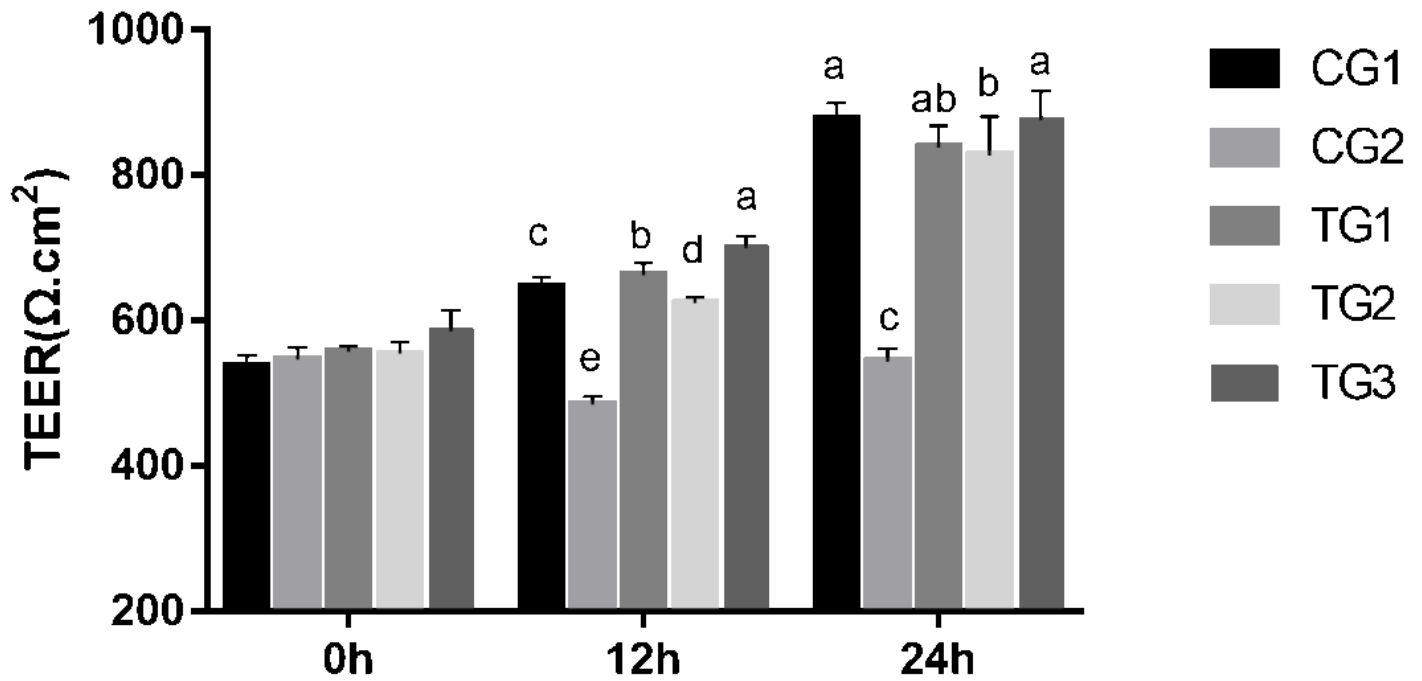
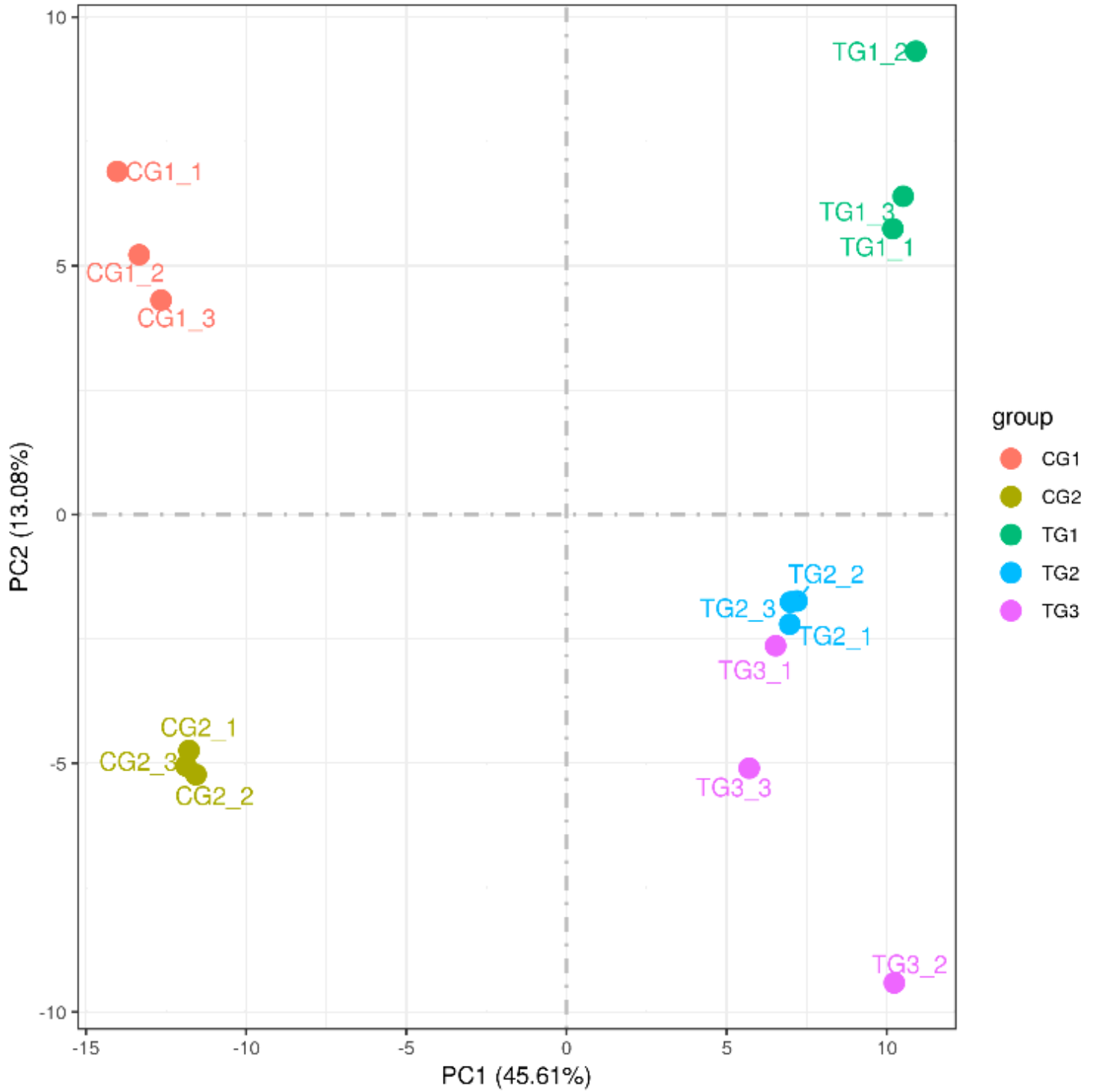


Figure 3

Effects of VA/RA on the TEER of IECs. VA/RA increases TEER of IECs monolayers subjected to an oxidative stress stimulus. Bars with different letters indicate significant difference (P < 0.05). Data are means  $\pm$  SD, n = 6, comparison between various groups by two-way ANOVA.



**Figure 4**

Principal component analysis result graph, the abscissa in the figure is the first principal component, and the ordinate is the second principal component.

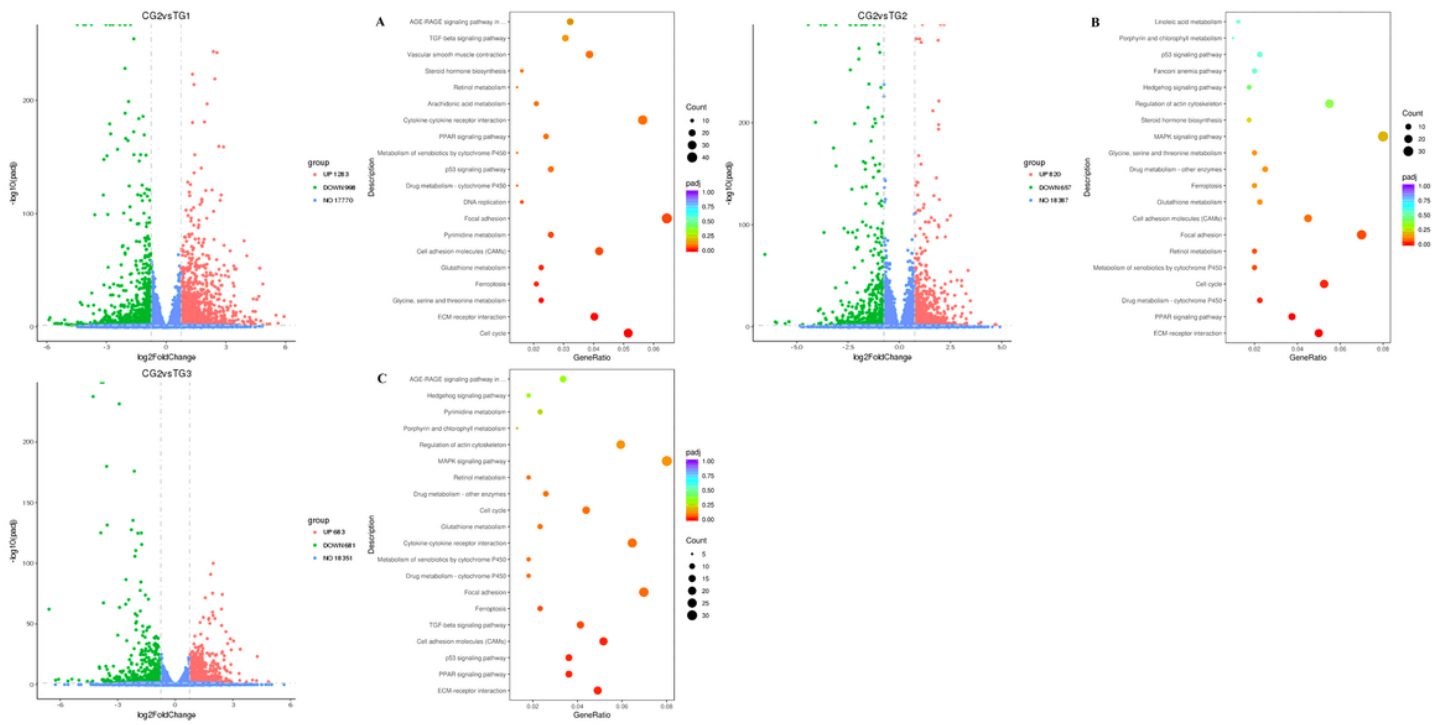


**Figure 5**

KEGG analysis of DEGs. (A) KEGG analysis of DEGs between CG2 and TG1 groups. (B) KEGG analysis of DEGs between CG2 and TG2 groups. (C) KEGG analysis of DEGs between CG2 and TG3 groups. DEGs: differentially expressed genes.

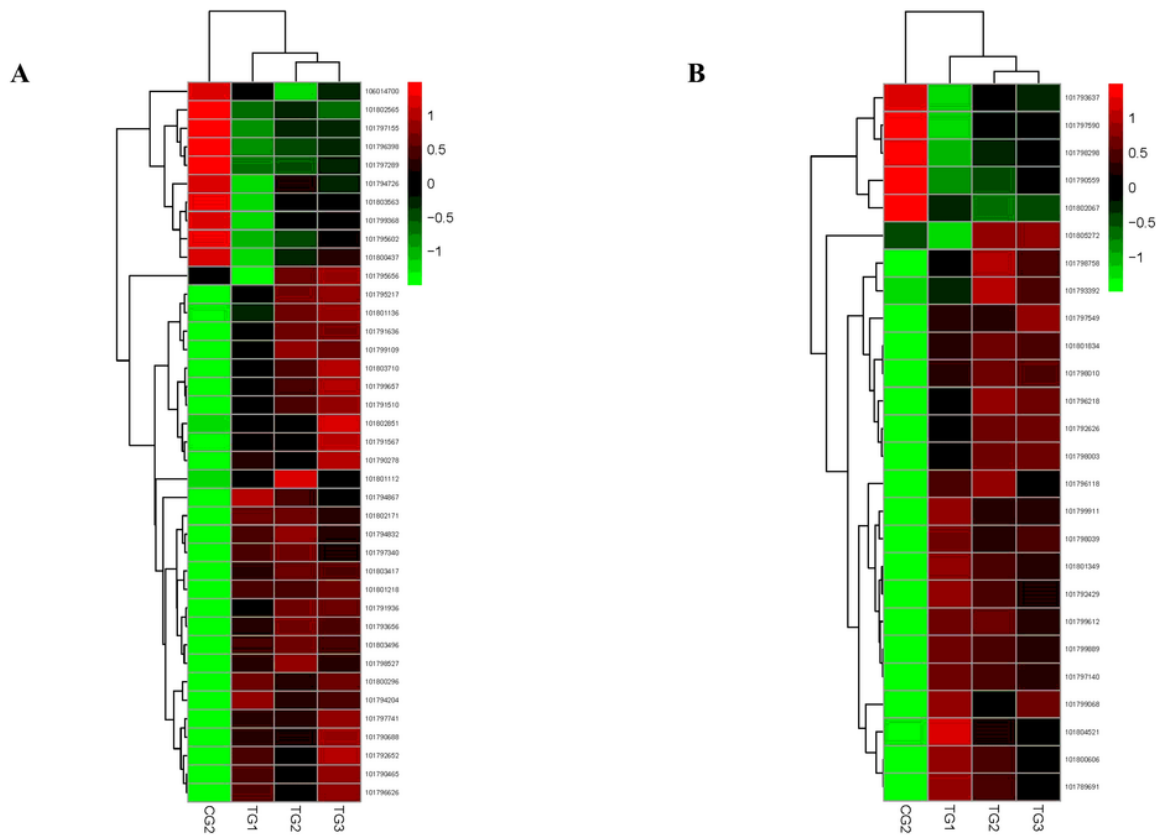


**Figure 6**

Differential expression genes in TGs and CG2. (A) Heat map of differential genes in cell adhesion molecules among TGs and CG2. (B) Heat map of differential expression genes in PPAR signaling pathway among TGs and CG2.

**Figure 7**

Real-time PCR verification of selected differentially expressed genes from the RNA-seq; PPAR $\gamma$ : peroxisome proliferator activated receptor-gamma; ACSL1: acid CoA ligase 1; ACSL5: long-chain fatty acid CoA ligase 5.

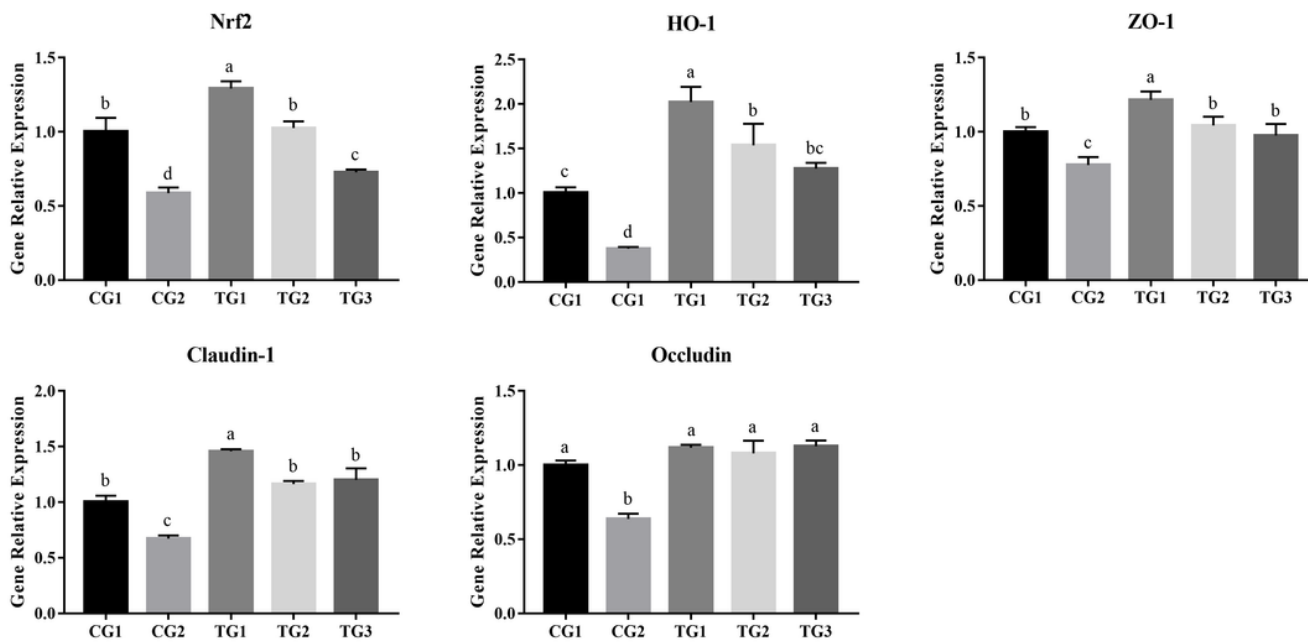


**Figure 8**

Effect of VA and its derivative RA on transcripts of anti-oxidative stress, endoplasmic reticulum stress and intestinal barrier related genes after oxidative stress induced by H<sub>2</sub>O<sub>2</sub>. Bars with different letters indicate significant difference (P < 0.05); Nrf2: nuclear factor (erythroid 2)-like 2; HO-1: heme oxygenase-1; ZO-1: zonula occludens-1.